Open Journal of
Discrete Applied Mathematics

PSR Press

Article

Sombor index and its applications

Vijaylaxmi S. Shigehalli[1,*] and Sammed A. Chougale[1]

1 Department of Mathematics, Rani Channamma University, Belagavi-591156
* Correspondence:shigehallivs@gmail.com

Received: 25 July 2024; Accepted: 04 October 2024; Published: 23 April 2025
Communicated by: Kamran Jamil

Abstract: A novel topological index, the Sombor index, has been proposed by Ivan Gutman in a recent paper [1]. Motivated by this novel index, we study the new variants of Sombor index and to examine the correlation of newly introduced topological indices we have computed the values of these indices by taking all possible trees on 10 vertices. Here in this paper, we derive explicit formulae for the Sombor index of various nanostructures. These include hexagonal parallelogram $P(\alpha,\beta)$-nanotubes, triangular benzenoid G_α, and zigzag-edge coronoid fused with starphene nanotubes $ZCS(k,\alpha,\beta)$, where k,α,β are natural numbers. We also compute the Sombor index for dominating derived networks D_1, D_2, D_3, as well as for various dendrimers such as Porphyrin Dendrimer, Ninc-Porphyrin Dendrimer, Propyl Ether Imine Dendrimers, and Polyamidoamin (PAMAM) Dendrimer. Additionally, we examine Polyamidoamin dendrimers (PD_1, PD_2, DS_1) and linear polyomino chains like L_α, Z_α, $B^1_\alpha(\alpha \geq 3), B^2_\alpha(\alpha \geq 4)$. Finally, we consider benzenoid systems with different shapes, including triangular, hourglass, and jagged-rectangle configurations. By computing the Sombor index for these nanostructures, we provide a comprehensive analysis of their topological properties.

Keywords: Sombor index, trees, nanostructures, dendrimers

MSC: 05C90, 05C35, 05C12.

1. Introduction

All graphs considered in this paper are finite, simple, and undirected, meaning they do not have loops. A graph Γ is defined as $\Gamma = (V, E)$, where $V(\Gamma) = \{v_1, v_2, v_3, \cdots, v_n\}$ is the vertex set and $E(\Gamma) = \{e_1, e_2, e_3, \cdots, e_m\}$ is the edge set, with $|V(\Gamma)| = n$ and $|E(\Gamma)| = m$. In graph Γ, two vertices u and v are adjacent if $uv \in E(\Gamma)$. The open neighborhood of a vertex $v \in V(\Gamma)$ is denoted as $N(v) = \{u : uv \in E(\Gamma)\}$, and the closed neighborhood is $N[v] = N(v) \cup \{v\}$. The degree of a vertex $v \in V(\Gamma)$ is represented as $d_\Gamma(v) = |N(v)|$. Vertices in Γ can be classified into three types: pendant vertices with $|N(v)| = 1$, support vertices adjacent to pendant vertices, and internal vertices with $|N(v)| > 1$. For any $r \in \mathbb{Z}^+$, a graph Γ with $deg(v) = r$ for every $v \in V(\Gamma)$ is called an r-regular graph. Specifically, if $r = 2$, Γ is called a cycle C_α; if $r = 3$, Γ is a cubic graph. If $|V| = |E|$, a graph Γ is said to be unicyclic. For any undefined terms, please refer to [2]. Molecular descriptors offer a guiding light in navigating the vast chemical space, transforming a potentially random search into a systematic exploration for substances crucial to human progress. Among various molecular descriptors, topological indices hold a prominent position. These indices are the numbers associated with molecular graphs, and numerous researchers have proposed a vast array of such quantities since 1972 [3].

A topological index is considered useful if it demonstrates strong predictive capabilities in Quantitative Structure-Property Relationship (QSPR) studies. Consequently, topological indices can be categorized into two groups: useful and less useful ones. The Sombor index, denoted as $SO(\Gamma)$, stands out as a particularly valuable topological index. Introduced by Ivan Gutman [1], the Sombor index has shown promising results in QSPR studies, making it a notable contribution to the field.

$$SO(\Gamma) \quad = \quad \sum_{uv \in E(\Gamma)} [\sqrt{d_\Gamma(u)^2 + d_\Gamma(v)^2}]. \tag{1}$$

Inspired by the Sombor index, we introduce new variants of this index, defined as:

$$SO'(\Gamma) = \sum_{uv\in E(\Gamma)} [\sqrt{d_\Gamma(u)^2 \times d_\Gamma(v)^2}], \tag{2}$$

$$N_{SO}(\Gamma) = \sum_{uv\in E(\Gamma)} [\sqrt{d_\Gamma(S(u))^2 + d_\Gamma(S(v))^2}], \tag{3}$$

$$N'_{SO}(\Gamma) = \sum_{uv\in E(\Gamma)} [\sqrt{d_\Gamma(S(u))^2 \times d_\Gamma(S(v))^2}], \tag{4}$$

where $d_\Gamma(S(u))$ denotes the cumulative degree of the vertices adjacent to u in graph Γ. For further details on topological indices, please consult the referenced literature [4–9].

2. Quality of sombor index and its variants

The concept of quality in topological descriptors has been a subject of varying interpretations among researchers. Efforts have been made to establish a unified framework and define a set of criteria that a novel topological invariant should meet. A prominent contribution to this endeavor is the Randic [10] set of qualities, widely recognized and cited in the field of chemical graph theory. Randic proposed a comprehensive list of thirteen tests that a novel topological index should undergo. Successfully passing these tests would qualify the index for further in-depth examination. The tests encompass both chemical and technical aspects, with the latter being universally satisfied by most topological indices. This framework provides a benchmark for evaluating the quality and validity of novel topological descriptors.

2.1. Relationships between Sombor index and its variants

The introduction of novel topological indices that are highly correlated with existing indices raises questions about their necessity, as most structural features of the underlying graph can be captured by existing invariants. Therefore, it is crucial to evaluate whether the correlations between a new descriptor and similar indices exceed acceptable limits. To address this, we calculated the topological indices for all trees with 10 vertices [2] and computed the Sombor index and its variants. The resulting correlations are presented below.

Table 1. Different variants of $SO(T)$ for non-isomorphic trees with 10 vertices

Tree	$SO(T)$	$SO'(T)$	$N_{SO}(T)$	$N'_{SO}(T)$
T_1	24.2711	32	45.495	116
T_2	26.3083	34	43.3822	130
T_3	25.7159	32	48.6852	129
T_4	26.1592	35	47.4309	122
T_5	26.0101	36	50.4726	140
T_6	26.1592	35	49.9902	141
T_7	26.0101	36	46.7485	151
T_8	26.0101	36	45.8926	140
T_9	30.3912	38	54.1498	164
T_{10}	30.1479	34	57.5761	182
T_{11}	29.7988	36	57.5229	189
T_{12}	29.9045	42	61.0732	202
T_{13}	29.9045	42	60.5761	208
T_{14}	28.0175	42	64.7709	222
T_{15}	36.5025	44	60.3884	200
T_{16}	36.1963	47	67.917	254

Tree	$SO(T)$	$SO'(T)$	$N_{SO}(T)$	$N'_{SO}(T)$
T_{17}	36.1963	47	68.0484	257
T_{18}	35.8901	50	73.3683	283
T_{19}	30.9559	44	78.8602	309
T_{20}	44.6312	52	97.0892	316
T_{21}	44.2807	56	81.3734	356
T_{22}	43.6883	54	79.6742	368
T_{23}	54.7710	62	88.9148	441
T_{24}	54.3876	67	97.5843	491
T_{25}	50.7935	58	106.2385	603
T_{26}	81.4984	81	114.55	729
T_{27}	26.4930	36	51.2693	144
T_{28}	25.4177	37	52.9866	152
T_{29}	28.1834	38	54.6509	163
T_{30}	28.0473	38	47.5545	136
T_{31}	28.6396	33	52.8837	155
T_{32}	28.1964	37	52.9320	156
T_{33}	28.0473	38	54.626	167
T_{34}	24.4417	38	54.6652	164
T_{35}	25.2188	32	56.3682	173
T_{36}	28.0473	38	54.6561	162
T_{37}	28.1964	37	56.4096	174
T_{38}	27.9072	39	56.4038	172
T_{39}	27.9072	39	56.3418	165
T_{40}	27.9072	39	56.3951	174
T_{41}	27.8982	39	58.1842	184
T_{42}	27.7582	40	56.9302	174
T_{43}	27.6091	41	58.7240	184
T_{44}	32.4284	40	57.0369	178
T_{45}	32.2793	37	60.0142	188
T_{46}	32.1850	42	60.3162	198
T_{47}	32.2793	41	58.7525	191
T_{48}	32.1850	42	60.5030	202
T_{49}	32.1302	42	60.3977	201
T_{50}	32.0359	43	62.2377	208
T_{51}	31.9417	44	63.9989	219
T_{52}	23.0972	40	63.0661	222
T_{53}	31.9358	44	63.7966	218
T_{54}	31.8809	44	63.9201	221
T_{55}	31.7867	45	65.6661	227
T_{56}	31.6924	46	67.4935	238
T_{57}	31.6376	46	67.5749	209
T_{58}	31.7867	45	65.8153	228
T_{59}	31.5434	47	69.3628	205
T_{60}	31.4491	44	103.586	255
T_{61}	38.5397	46	65.4695	241
T_{62}	38.3906	47	67.3811	251
T_{63}	38.2335	49	67.7562	251
T_{64}	38.0593	46	72.4539	281
T_{65}	37.9022	52	76.0151	301
T_{66}	37.9102	51	62.7295	216

Tree	$SO(T)$	$SO'(T)$	$N_{SO}(T)$	$N'_{SO}(T)$
T_{67}	32.3679	53	76.9612	308
T_{68}	37.5960	55	81.5069	327
T_{69}	56.5985	54	77.3483	333
T_{70}	46.1259	59	85.8494	383
T_{71}	45.9244	62	91.0780	413
T_{72}	56.3667	69	100.112	513
T_{73}	36.5113	44	62.5245	216
T_{74}	36.2680	46	66.2609	236
T_{75}	35.5656	52	76.7989	293
T_{76}	35.5656	52	76.7290	252
T_{77}	35.8090	50	73.0192	276
T_{78}	42.6226	50	71.5626	279
T_{79}	41.5954	58	85.1560	271
T_{80}	43.4196	59	86.9025	333
T_{81}	49.9942	66	96.3577	459
T_{82}	47.8632	65	91.1115	441
T_{83}	29.8044	42	61.0622	201
T_{84}	29.2120	40	61.5342	200
T_{85}	31.2186	42	61.0545	197
T_{86}	29.6553	43	62.7823	207
T_{87}	29.6553	43	63.1326	205
T_{88}	29.9444	41	59.2292	191
T_{89}	29.9444	41	59.1821	187
T_{90}	29.9444	41	59.2813	188
T_{91}	30.0935	40	57.4647	177
T_{92}	30.2335	39	45.8736	177
T_{93}	32.9525	52	73.9957	271
T_{94}	33.5746	49	72.0852	237
T_{95}	33.9730	46	66.7222	235
T_{96}	28.1170	47	68.6798	245
T_{97}	33.6838	48	70.3820	239
T_{98}	33.7781	47	68.5687	242
T_{99}	34.1764	44	63.2115	215
T_{100}	34.0672	45	64.8992	225
T_{101}	43.4815	61	84.1534	345
T_{102}	37.9009	51	74.3867	279
T_{103}	37.5969	54	79.2030	309
T_{104}	31.7015	45	65.8726	225
T_{105}	31.7015	45	65.6594	221
T_{106}	39.9565	53	77.2554	305

The subsequent diagrams illustrate the relation between the Sombor index and its variants:

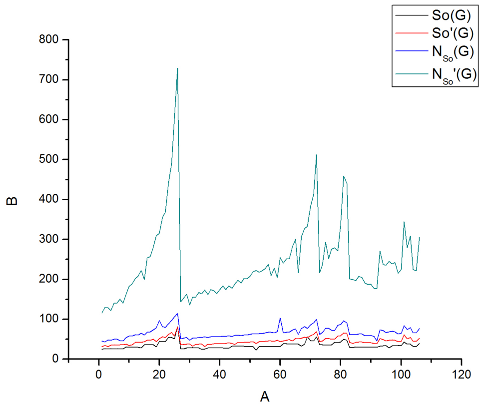
So(G)
So'(G)
$N_{So}(G)$
$N_{So}'(G)$
A
B

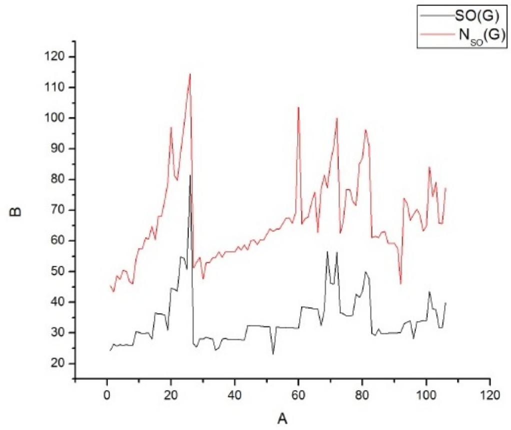
SO(G)
$N_{SO}(G)$
A
B

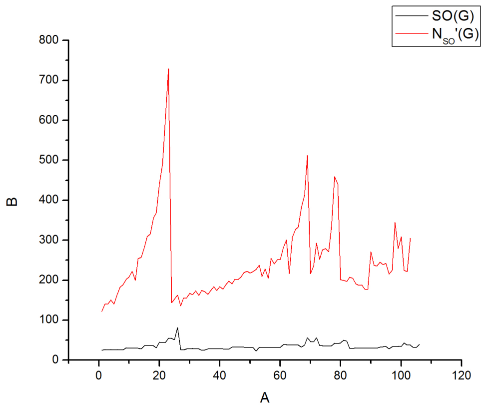
SO(G)
$N_{SO}'(G)$
A
B

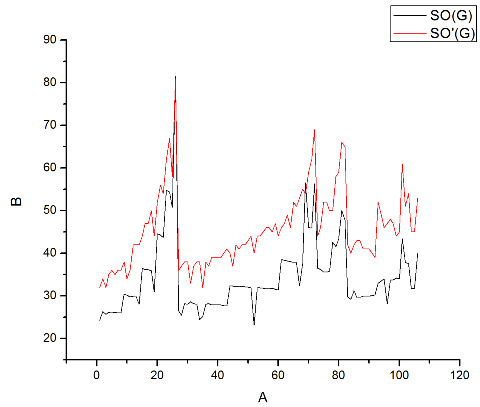
SO(G)
SO'(G)
A
B

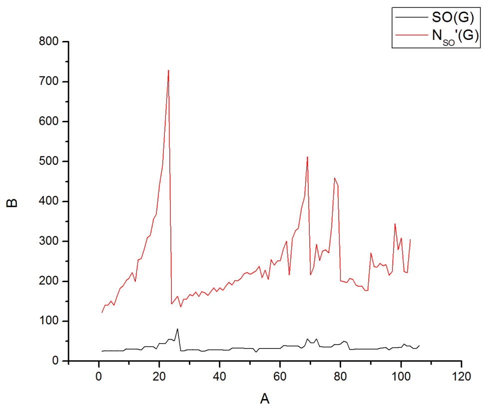
SO(G)
$N_{SO}'(G)$
A
B

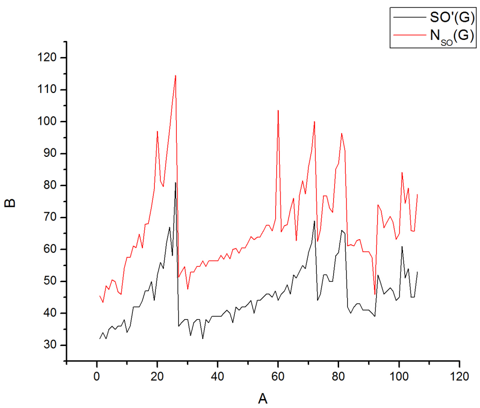
SO'(G)
$N_{SO}(G)$
A
B

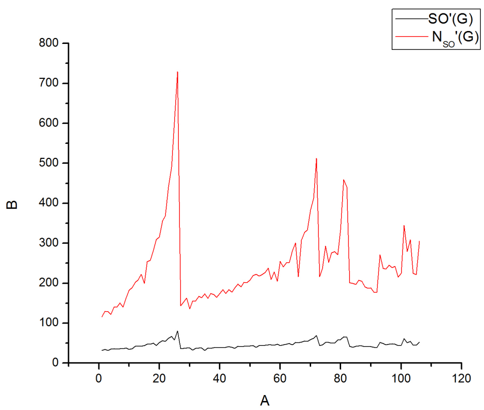
SO'(G)
$N_{SO}'(G)$
A
B

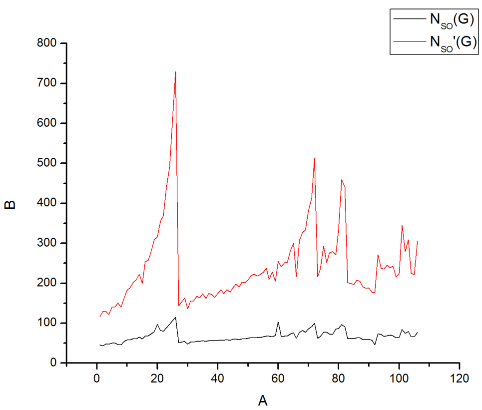
$N_{SO}(G)$
$N_{SO}'(G)$
A
B

The diagrams and Table 1 reveal that the Sombor index has limited correlation with its variants, implying that these variants may be valuable for QSPR analysis. This is because the variants may capture unique structural information not present in the original Sombor index, making them worth investigating for their predictive potential in QSPR studies.

3. Applications

This section explores the chemical structures of various nanotubes and dendrimers, including $P(\alpha,\beta)$-nanotubes, triangular benzenoid G_α, zigzag-edge coronoids fused with starphene nanotubes $ZCS(k,l,m)$ [11], dominating derived networks D_1, D_2, D_3 [12], porphyrin dendrimers, zinc-porphyrin dendrimers, propyl ether imine dendrimers, poly(ethylene amido amine) dendrimers, PAMAM dendrimers (PD_1, PD_2, DS_1) [13], linear polyomino chains $L_\alpha, Z_\alpha, B^1_\alpha(n \geq 3), B^2_\alpha(n \geq 4)$ [14], and benzenoid systems (triangular, hourglass, and jagged-rectangle) [15]. The explicit formulas for these structures are obtained and depicted in the following figures.

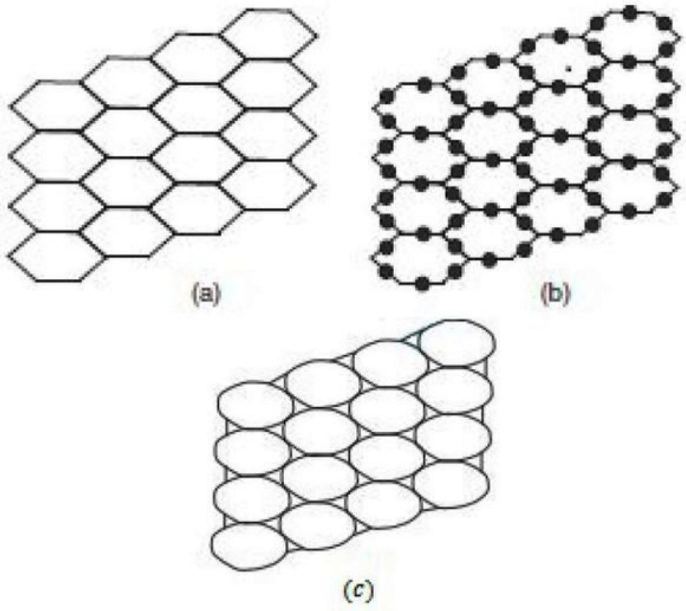

Figure 1. (a) $\mathcal{P}(4,4)$, (b) $S(\mathcal{P}(4,4))$, (c) $L(S(\mathcal{P}(4,4)))$

Theorem 1. *The $SO(L(S(P(\alpha,\beta)))$ is given by*

$$\begin{aligned} SO(\Gamma) &= 2\sqrt{8}(\alpha+\beta+4) + 4\sqrt{13}(\alpha+\beta-2) + \sqrt{18}(9\alpha\beta - 2m - 2n - 5), \\ SO'(\Gamma) &= 8(\alpha+\beta+4) + 24\sqrt{13}(\alpha+\beta-2) + 9(9\alpha\beta - 2m - 2n - 5). \end{aligned}$$

Proof. Let $P(\alpha,\beta)$; where α,β are positive integers, be the hexagonal parallelogram of order $2(\alpha+\beta+\alpha\beta)$ and size $(3\alpha\beta+2\alpha+2\beta+1)$ respectively and $G = L(S(P(\alpha,\beta)))$ be the line graph of the sub-division graph of $P(\alpha,\beta)$ implies, the points and lines of Γ are $2(3\alpha\beta+2\alpha+2\beta+1)$ and $9\alpha\beta+4\alpha+4\beta+5$ respectively. Let the subsets $\varpi_{2,2}, \varpi_{2,3}$ and $\varpi_{3,3}$, of the edge set of Γ can form a partition where $\varpi(L(S(P(\alpha,\beta)))) = \varpi_{2,2} \cup \varpi_{2,3} \cup \varpi_{3,3}$. Furthermore, $|\varpi_{2,2}| = 2(\alpha+\beta+4)$, $|\varpi_{2,3}| = 4(\alpha+\beta-2)$, $|\varpi_{3,3}| = 9\alpha\beta - 2\alpha - 2\beta - 5$. Such that $|\varpi(L(S(P(\alpha,\beta))))| = |\varpi_{2,2}| + |\varpi_{2,3}| + |\varpi_{3,3}| = 9\alpha\beta + 4\alpha + 4\beta + 5$. Therefore, employing Eqs. (1)-(2), we obtain the desired result. □

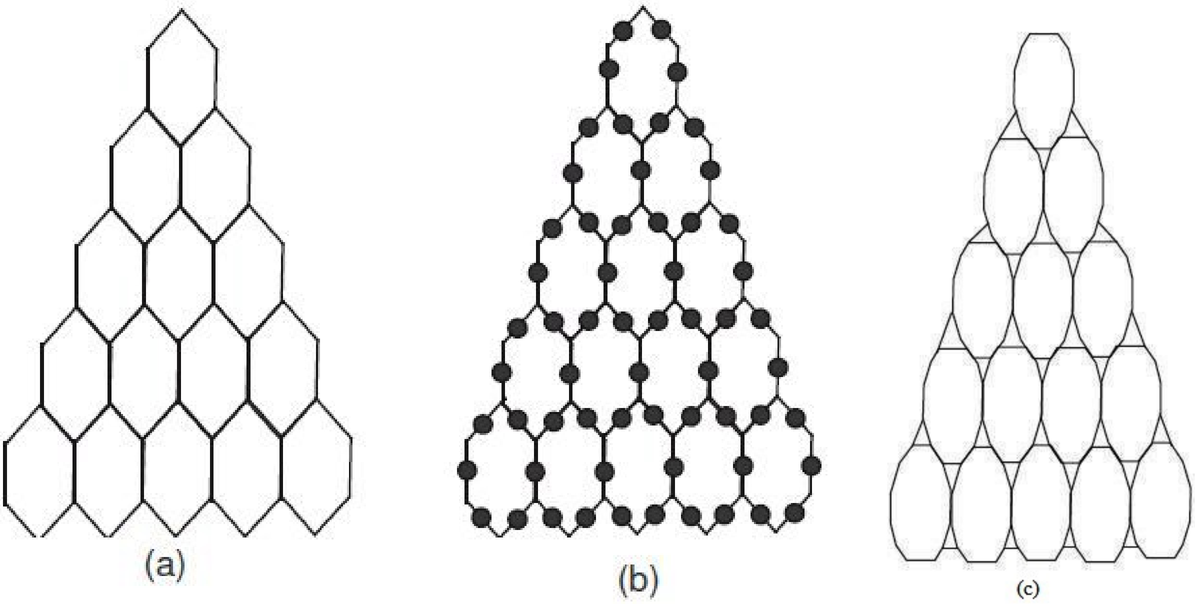

Figure 2. (a) G_5 (b) $S(G_5)$ (c) $L(S(G_5))$

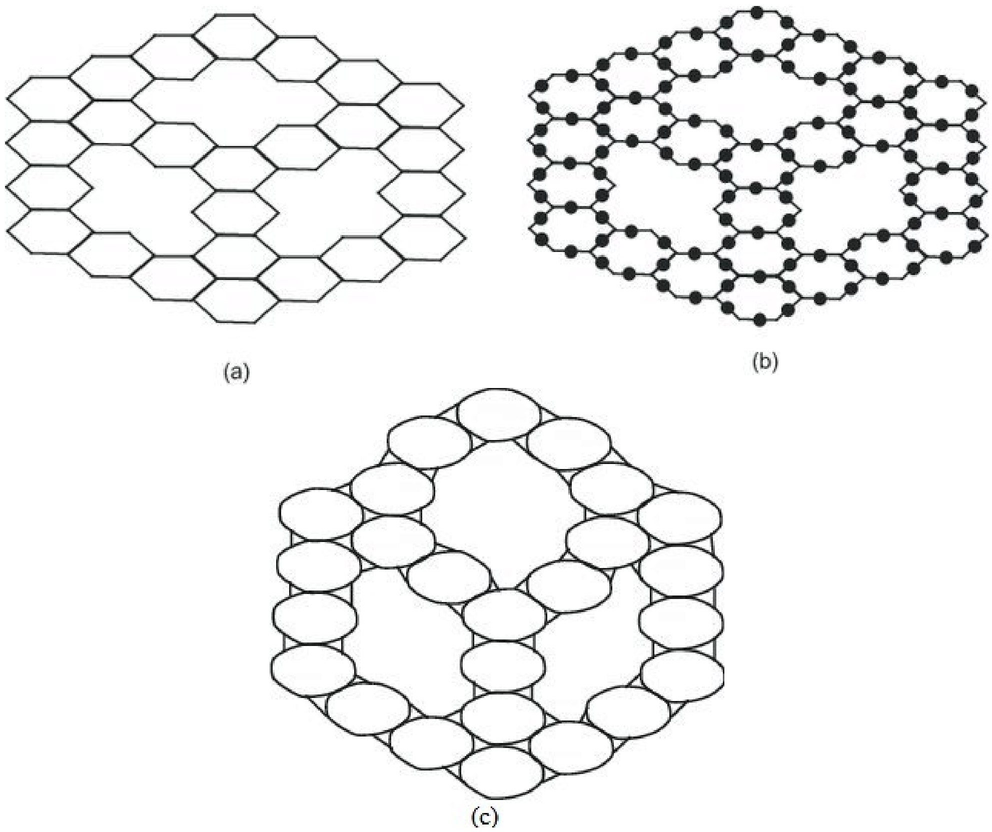

Figure 3. (a) $\mathcal{ZCS}(4,4,4)$ (b) $S(\mathcal{ZCS}(4,4,4))$ (c) $L(S(\mathcal{ZCS}(4,4,4)))$

Theorem 2. *The $SO(L(S(G_\alpha)))$ is given by*

$$\begin{aligned} SO(\Gamma) &= 3\sqrt{8}(\alpha+3) + 6\sqrt{13}(\alpha-1) + 3\sqrt{18}\frac{3\alpha^2+\alpha-4}{2}, \\ SO'(\Gamma) &= 12(\alpha+3) + 36(\alpha-1) + 27\frac{3\alpha^2+\alpha-4}{2}. \end{aligned}$$

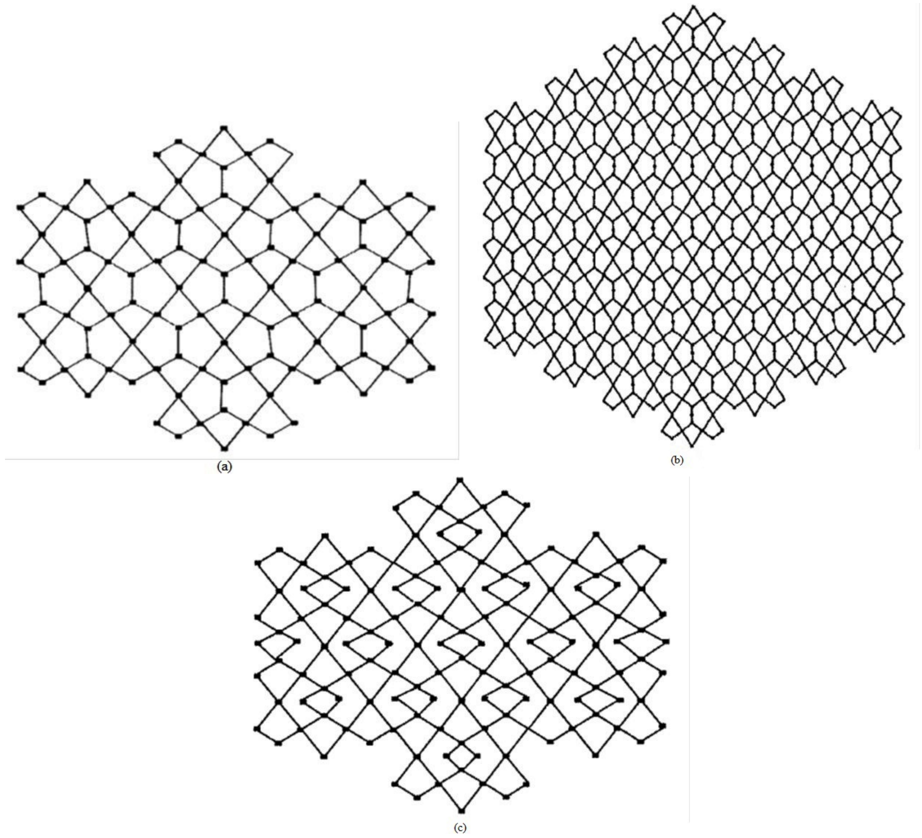

Figure 4. (a) Dominating derived network of 1st type $D_1(2)$, (b) Dominating derived network of 2nd type $D_2(4)$, (c)Dominating derived network of 3rd type $D_3(n)$

Proof. Consider the triangular benzenoid graph G_α of order $\alpha^2 + 4\beta + 1$ and size $\frac{3}{2}\alpha(\alpha + 3)$, where α is a positive integer. Let $L(S(G_\alpha))$ denote the line graph of the sub-division graph of G_α. Then, the points and lines of $L(S(G_\alpha))$ are $3\alpha(\alpha + 3)$ and $\frac{3(3\alpha^2+7\alpha+2)}{2}$, respectively. Let the subsets $\varpi_{2,2}, \varpi_{2,3}$ and $\varpi_{3,3}$, of the edge set of Γ can form a partition where $\varpi(L(S(G_\alpha))) = \varpi_{2,2} \cup \varpi_{2,3} \cup \varpi_{3,3}$ Furthermore, $|\varpi_{2,2}| = 3(\alpha + 3)$, $|\varpi_{2,3}| = 6(\alpha - 1)$, $|\varpi_{3,3}| = \frac{3(3\alpha^2+\alpha-4)}{2}$. Where $|\varpi(L(S(G_\alpha)))| = |\varpi_{2,2}| + |\varpi_{2,3}| + |\varpi_{3,3}| = \frac{3(3\alpha^2+7\alpha+2)}{2}$. Therefore, employing Eqs. (1)-(2), we obtain the desired result. □

Theorem 3. *The $SO(L(S(ZCS(k, \alpha, \beta))))$ is given by*

$$SO(\Gamma) = 6\sqrt{8}(k + \alpha + \beta - 5) + 12\sqrt{13}(k + \alpha + \beta - 7) + 21\sqrt{18}((k + \alpha + \beta) - 39),$$
$$SO'(\Gamma) = 24(k + \alpha + \beta - 5) + 72(k + \alpha + \beta - 7) + 189\sqrt{18}((k + \alpha + \beta) - 39).$$

Proof. Consider the zigzag-edge coronoid fused with starphene nanotubes $ZCS(k, \alpha, \beta)$, where $k = \alpha = \beta = 4$. Let I denote this graph, which has order $36k + 54$ and size $15(k + \alpha + \beta) - 63$. Let $L(S(I))$ be the line graph of the subdivision graph of I. Then, the points and lines of $L(S(I))$ are $30(k + \alpha + \beta) - 126$ and $39(k + \alpha + \beta) + 153$, respectively.

The three disjoint sets: $\varpi_{2,2}, \varpi_{2,3}$, and $\varpi_{3,3}$ form a partition for $\varpi(L(S(I)))$, where $\varpi(L(S(I))) = \varpi_{2,2} \cup \varpi_{2,3} \cup \varpi_{3,3}$. Furthermore, we have:

$$|\varpi_{2,2}| = 6(k + \alpha + \beta - 5),$$
$$|\varpi_{2,3}| = 12(k + \alpha + \beta - 7),$$
$$|\varpi_{3,3}| = 21(k + \alpha + \beta) - 39.$$

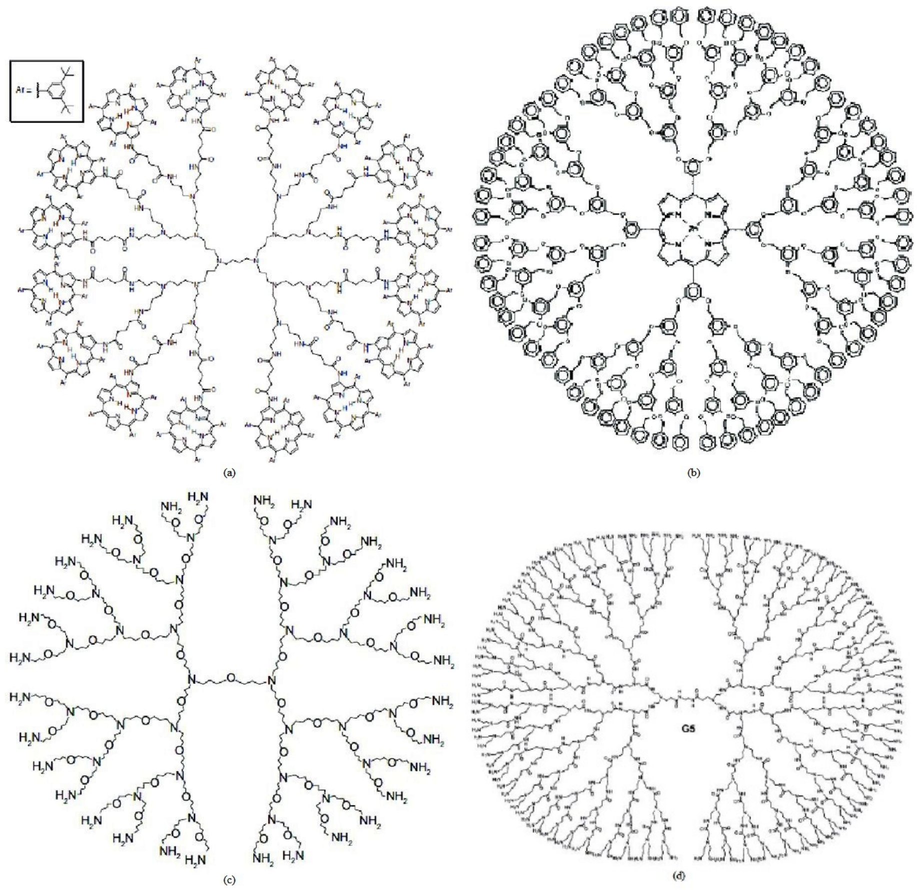

Figure 5. Various kinds of Dendrimers

Thus, we have $|\varpi(L(S(I)))| = |\varpi_{2,2}| + |\varpi_{2,3}| + |\varpi_{3,3}| = 39(k+\alpha+\beta) + 153 = 405$. Therefore, employing Eqs. (1)-(2), we obtain the desired result. □

Theorem 4. *The $SO(D_1(\alpha))$ is given by*

$$\begin{aligned} SO(D_1(\alpha)) &= 4\sqrt{8}\alpha + \sqrt{13}(4\beta - 4) + \sqrt{20}(28\alpha - 16) + \sqrt{18}(9\alpha^2 - 13\alpha + 5) \\ &\quad +5(36\alpha^2 - 56\alpha + 24) + \sqrt{32}(36\alpha^2 - 52\alpha + 20), \\ SO'(D_1(n)) &= \frac{49}{100}\alpha^2 + \frac{19}{25}\alpha - \frac{8}{25}. \end{aligned}$$

Proof. Consider the dominating derived network of the first type, denoted by $D_1(\alpha)$. The six mutually disjoint subsets namely $\varpi_{2,2}, \varpi_{2,3}, \varpi_{2,4}, \varpi_{3,3}, \varpi_{3,4}$ and $\varpi_{4,4}$ can form the partition of the set $\varpi(D_1(\alpha))$ where $\varpi(D_1(\alpha)) = \varpi_{2,2} \cup \varpi_{2,3} \cup \varpi_{2,4} \cup \varpi_{3,3} \cup \varpi_{3,4} \cup \varpi_{4,4}$. Further, $|\varpi_{2,2}| = 4\beta$, $|\varpi_{2,3}| = 4\beta - 4$, $|\varpi_{2,4}| = 28\alpha - 16$, $|\varpi_{3,3}| = 9\alpha^2 - 13\alpha + 5$, $|\varpi_{3,4}| = 36\alpha^2 - 56\alpha + 24$ and $|\varpi_{4,4}| = 36\alpha^2 - 52\alpha + 20$. Such that $|\varpi(D_1(n))| = |\varpi_{2,2}| + |\varpi_{2,3}| + |\varpi_{2,4}| + |\varpi_{3,3}| + |\varpi_{3,4}| + |\varpi_{4,4}|$. Thus, employing Eqs. (1)-(2), we get the required result. □

Theorem 5. *The $SO(D_2(\alpha)))$ is given by*

$$\begin{aligned} SO(D_2(n)) &= 4\sqrt{8}\alpha + \sqrt{13}(18\alpha^2 - 22\alpha + 6) + \sqrt{20}(28\alpha - 16) + 5(36\alpha^2 - 56\alpha + 24) \\ &\quad +\sqrt{32}(36\alpha^2 - 52\alpha + 20), \\ SO'(D_2(n)) &= 16\alpha + 6(18\alpha^2 - 22\alpha + 6) + 8(28\alpha - 16) + 12(36\alpha^2 - 56\alpha + 24) \\ &\quad +16(36\alpha^2 - 52\alpha + 20). \end{aligned}$$

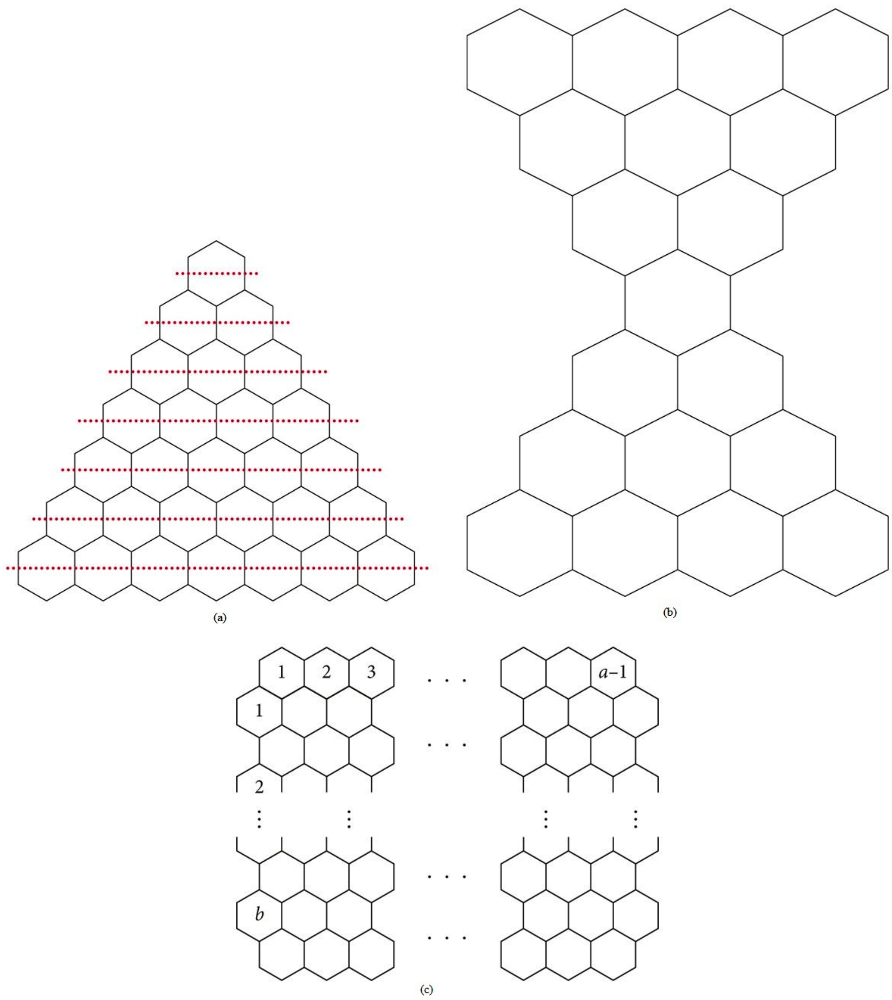

Figure 6. Three different types of Benzoid systems

Proof. Consider the dominating derived network of the 2nd type, denoted by $D_2(\alpha)$. The five mutually disjoint subsets namely $\varpi_{2,2}, \varpi_{2,3}, \varpi_{2,4}, \varpi_{3,4}$ and $\varpi_{4,4}$ can form the partition of the set $\varpi(D_2(\alpha))$ where $\varpi(D_2(\alpha)) = \varpi_{2,2} \cup \varpi_{2,3} \cup \varpi_{2,4} \cup \varpi_{3,4} \cup \varpi_{4,4}$. Further, $|\varpi_{2,2}| = 4\beta$, $|\varpi_{2,3}| = 18\alpha^2 - 22\alpha + 6$, $|\varpi_{2,4}| = 28\alpha - 16$, $|\varpi_{3,4}| = 36\alpha^2 - 56\alpha + 24$ and $|\varpi_{4,4}| = 36\alpha^2 - 52\alpha + 20$. Such that $|\varpi(D_2(\alpha))| = |\varpi_{2,2}| + |\varpi_{2,3}| + |\varpi_{2,4}| + |\varpi_{3,4}| + |\varpi_{4,4}|$. Thus, employing Eqs. (1)-(2), we get the required result. □

Theorem 6. *The $SO(D_3(\alpha))$ is given by*

$$\begin{aligned} SO(D_3(n)) &= 4\sqrt{8}\alpha + \sqrt{20}(36\alpha^2 - 20\alpha) + \sqrt{32}(72\alpha^2 - 108\alpha + 44), \\ SO'(D_3(n)) &= 16\alpha + 8(36\alpha^2 - 20n) + 16(72\alpha^2 - 108\alpha + 44). \end{aligned}$$

Proof. Consider the dominating derived network of the 3rd type, denoted by $D_3(\alpha)$. The three mutually disjoint subsets namely $\varpi_{2,2}, \varpi_{2,4}$ and $\varpi_{4,4}$ can form the partition of the set $\varpi(D_3(\alpha))$, where $\varpi(D_3(\alpha)) = \varpi_{2,2} \cup \varpi_{2,4} \cup \varpi_{4,4}$. Further, $|\varpi_{2,2}| = 4\beta$, $|\varpi_{2,4}| = 36\alpha^2 - 20\alpha$ and $|\varpi_{4,4}| = 72\alpha^2 - 108\alpha + 44$. Such that $|\varpi(D_3(\alpha))| = |\varpi_{2,2}| + |\varpi_{2,4}| + |\varpi_{4,4}|$. Therefore, using Eqs. (1)-(2), we arrive at the desired result. □

Theorem 7. *The $SO(D_\alpha P_\alpha)$ is given by*

$$\begin{aligned} SO(D_\alpha P_\alpha) &= 2\sqrt{10}\alpha + 24\sqrt{17}\alpha + \sqrt{8}(10\alpha - 5) + \sqrt{13}(48\alpha - 6) + 13\sqrt{18}\alpha + 40\alpha, \\ SO'(D_\alpha P_\alpha) &= 315\alpha + 4(10\alpha - 5) + 6(48\alpha - 6). \end{aligned}$$

Proof. Consider the prophyrin dendrimer $D_\alpha P_\alpha$ of order $96\alpha - 10$ and size $105\alpha - 11$, respectively. The six mutually disjoint subsets namely; $\varpi_{1,3}, \varpi_{1,4}, \varpi_{2,2}, \varpi_{2,3}, \varpi_{3,3}$, and $\varpi_{3,4}$ can form the partition of the set $\varpi(D_\alpha P_\alpha)$ such that $\varpi(D_\alpha P_\alpha) = \varpi_{1,3} \cup \varpi_{1,4} \cup \varpi_{2,2} \cup \varpi_{2,3} \cup \varpi_{3,3} \cup \varpi_{3,4}$ Furthermore, we have $|\varpi_{1,3}| = 2\alpha$, $|\varpi_{1,4}| = 24\alpha$, $|\varpi_{2,2}| = 10\alpha - 5$, $|\varpi_{2,3}| = 48n - 6$, $|\varpi_{3,3}| = 13\alpha$, and $|\varpi_{3,4}| = 8\alpha$. Thus, we obtain $|\varpi(D_\alpha P_\alpha)| = |\varpi_{1,3}| + |\varpi_{1,4}| + |\varpi_{2,2}| + |\varpi_{2,3}| + |\varpi_{3,3}| + |\varpi_{3,4}| = 105\alpha - 11$. Therefore, using Eqs. (1)-(2), we arrive at the desired result. □

Theorem 8. *The $SO(DPZ_\alpha)$ is given by*

$$\begin{aligned} SO(DPZ_\alpha) &= 16\sqrt{8} \cdot 2^\alpha + \sqrt{13}(40 \cdot 2^\alpha - 16) + \sqrt{18}(8 \cdot 2^\alpha - 16) + 20, \\ SO'(DPZ_\alpha) &= 64 \cdot 2^\alpha + 6(40 \cdot 2^\alpha - 16) + 9(8 \cdot 2^\alpha - 16) + 48. \end{aligned}$$

Proof. Let DPZ_α be the Zinc-Porphyrin dendrimer of order $96\alpha - 10$ and size $105\alpha - 11$, respectively. The four mutually disjoint subssets $\varpi_{2,2}, \varpi_{2,3}, \varpi_{3,3}$, and $\varpi_{3,4}$ can form the partition of $\varpi(DPZ_\alpha)$ such that $\varpi(DPZ_\alpha) = \varpi_{2,2} \cup \varpi_{2,3} \cup \varpi_{3,3} \cup \varpi_{3,4}$. Furthermore, we have $|\varpi_{2,2}| = 16 \cdot 2^\alpha - 4$, $|\varpi_{2,3}| = 40 \cdot 2^\alpha - 16$, $|\varpi_{3,3}| = 8 \cdot 2^\alpha - 16$, and $|\varpi_{3,4}| = 4$ Thus, we obtain $|\varpi(DPZ_\alpha)| = |\varpi_{2,2}| + |\varpi_{2,3}| + |\varpi_{3,3}| + |\varpi_{3,4}| = 105\alpha - 11$. Therefore, using Eqs. (1)-(2), we arrive at the desired result. □

Theorem 9. *The $SO(PD_1)$ is given by*

$$\begin{aligned} SO(PD_1) &= 3\sqrt{5} \cdot 2^\alpha + \sqrt{10}(6 \cdot 2^\alpha - 3) + \sqrt{8}(18 \cdot 2^\alpha - 9) + \sqrt{13}(21 \cdot 2^\alpha - 12), \\ SO'(PD_1) &= 6 \cdot 2^\alpha + 3(6 \cdot 2^\alpha - 3) + 4(18 \cdot 2^\alpha - 9) + 6(21 \cdot 2^\alpha - 12). \end{aligned}$$

Proof. Consider the PAMAM dendrimer PD_1 built from a triple-functional core unit and generated through a stepwise growth process, G_α, that is repeated α times. The four mutually disjoint subsets $\varpi_{1,2}, \varpi_{1,3}, \varpi_{2,2}$, and $\varpi_{2,3}$ can form a partition for $\varpi(PD_1)$, such that $\varpi(PD_1) = \varpi_{1,2} \cup \varpi_{1,3} \cup \varpi_{2,2} \cup \varpi_{2,3}$. Further, $|\varpi_{1,2}| = 3 \cdot 2^\alpha$, $|\varpi_{1,3}| = 6 \cdot 2^\alpha - 3$, $|\varpi_{2,2}| = 18 \cdot 2^\alpha - 9$ and $|\varpi_{2,3}| = 21 \cdot 2^\alpha - 12$. Such that $|\varpi(PD_1)| = |\varpi_{1,2}| + |\varpi_{1,3}| + |\varpi_{2,2}| + |\varpi_{2,3}$. Therefore, using Eqs. (1)-(2), we arrive at the desired result. □

Theorem 10. *The $SO(PD_2)$ is given by*

$$\begin{aligned} SO(PD_2) &= 4\sqrt{5} \cdot 2^\alpha + \sqrt{10}(8 \cdot 2^\alpha - 4) + \sqrt{8}(24 \cdot 2^\alpha - 11) + \sqrt{13}(28 \cdot 2^\alpha - 14), \\ SO'(PD_2) &= 8 \cdot 2^\alpha + 3(8 \cdot 2^\alpha - 4) + 4(24 \cdot 2^\alpha - 11) + 6(28 \cdot 2^\alpha - 14). \end{aligned}$$

Proof. Consider the PAMAM dendrimer PD_2 built from a triple-functional core unit and generated through a stepwise growth process, G_α, that is repeated α times. The four mutually disjoint subsets $\varpi_{1,2}, \varpi_{1,3}, \varpi_{2,2}$, and $\varpi_{2,3}$ can form a partition for $\varpi(PD_2)$, such that $\varpi(PD_2) = \varpi_{1,2} \cup \varpi_{1,3} \cup \varpi_{2,2} \cup \varpi_{2,3}$. Further, $|\varpi_{1,2}| = 4 \cdot 2^\alpha$, $|\varpi_{1,3}| = 8 \cdot 2^\alpha - 4$, $|\varpi_{2,2}| = 24 \cdot 2^\alpha - 11$ and $|\varpi_{2,3}| = 28 \cdot 2^\alpha - 14$. Such that $|\varpi(PD_2)| = |\varpi_{1,2}| + |\varpi_{1,3}| + |\varpi_{2,2}| + |\varpi_{2,3}$. Therefore, using Eqs. (1)-(2), we arrive at the desired result. □

Theorem 11. *The $SO(DS_1)$ is given by*

$$\begin{aligned} SO(DS_1) &= 4\sqrt{17} \cdot 3^\alpha + \sqrt{8}(10 \cdot 3^\alpha - 10) + \sqrt{20}(4 \cdot 3^\alpha - 4), \\ SO'(DS_1) &= 16\sqrt{17} \cdot 3^\alpha + 4(10 \cdot 3^\alpha - 10) + 8(4 \cdot 3^\alpha - 4). \end{aligned}$$

Proof. Consider the PAMAM dendrimer DS_1 built from a triple-functional core unit and generated through a stepwise growth process, G_α, that is repeated α times. The three mutually disjoint subsets $\varpi_{1,4}, \varpi_{2,2}$, and $\varpi_{2,4}$ can form a partition for $\varpi(DS_1)$, such that $\varpi(DS_1) = \varpi_{1,4} \cup \varpi_{2,2} \cup \varpi_{2,4}$. Further, $|\varpi_{1,4}| = 4 \cdot 3^n$, $|\varpi_{2,2}| = 10 \cdot 3^\alpha - 10$, and $|\varpi_{2,4}| = 4 \cdot 3^\alpha - 4$. Such that $|\varpi(DS_1)| = |\varpi_{1,4}| + |\varpi_{2,2}| + |\varpi_{2,4}|$. Therefore, using Eqs. (1)-(2), we arrive at the desired result. □

Theorem 12. *The $SO(L_\alpha)$ is given by*

$$\begin{aligned} SO(L_\alpha) &= 2\sqrt{8} + 4\sqrt{13} + \sqrt{18}(3\alpha - 5), \\ SO'(L_\alpha) &= 9(3\alpha - 5) + 32. \end{aligned}$$

Proof. Let L_α be the polyomino chain with n squares where $l_1 = \alpha$ and $\beta = 1$. The three mutually disjoint subsets $\varpi_{2,2}, \varpi_{2,3}$, and $\varpi_{3,3}$ can form a partition for $\varpi(L_\alpha)$, such that $\varpi(L_\alpha) = \varpi_{2,2} \cup \varpi_{2,3} \cup \varpi_{3,3}$. Further, $|\varpi_{2,2}| = 2$, $|\varpi_{2,3}| = 4$, and $|\varpi_{3,3}| = 3\alpha - 5$. Such that $|\varpi(L_\alpha)| = |\varpi_{2,2}| + |\varpi_{2,3}| + |\varpi_{3,3}|$. Therefore, using Eqs. (1)-(2), we arrive at the desired result. □

Theorem 13. *The $SO(Z_\alpha)$ is given by*

$$\begin{aligned} SO(Z_\alpha) &= 2\sqrt{20}(\beta - 1) + \sqrt{32}(3\alpha - 2\beta - 5) + 10 + 2\sqrt{8} + 4\sqrt{13}, \\ SO'(Z_\alpha) &= 16(\beta - 1) + 16(3\alpha - 2\beta - 5) + 32. \end{aligned}$$

Proof. Consider the zigzag polyomino chain Z_α consisting of α squares, where each segment S_i has length $l_i = 2$ and $\beta = \alpha - 1$. The polyomino chain is composed of a sequence of segments $S_1, S_2, \ldots, S_\beta$, where $\beta \geq 1$ and $i \in \{1, 2, \ldots, \beta\}$. The five mutually disjoint subsets $\varpi_{2,2}, \varpi_{2,3}$, $\varpi_{2,4}$, $\varpi_{3,4}$ and $\varpi_{4,4}$ can form a partition for $\varpi(Z_\alpha)$, such that $\varpi(Z_\alpha) = \varpi_{2,2} \cup \varpi_{2,3} \cup \varpi_{2,4} \cup \varpi_{3,4} \cup \varpi_{4,4}$. Further, $|\varpi_{2,2}| = 2$, $|\varpi_{2,3}| = 4$, $|\varpi_{2,4}| = 2(\beta - 1)$, $|\varpi_{3,4}| = 2$ and $|\varpi_{4,4}| = 3\alpha - 2\beta - 5$. Such that $|\varpi(Z_\alpha)| = |\varpi_{2,2}| + |\varpi_{2,3}| + |\varpi_{2,4}| + |\varpi_{3,4}| + |\varpi_{4,4}|$. Therefore, using Eqs. (1)-(2), we arrive at the desired result. □

Theorem 14. *Consider the polyomino chain B^1_α with α squares and β segments, where $\beta = 2$ and $S1$ and S_2 are the two segments satisfying $l_1 = 2$ and $l_2 = \alpha - 1$, respectively, for $\alpha \geq 3$. Then, we have the following*

$$\begin{aligned} SO(B^1_\alpha) &= \sqrt{18}(3\alpha - 10) + 2\sqrt{8} + 5\sqrt{13} + \sqrt{20} + 15, \\ SO'(B^1_\alpha) &= 9(3\alpha - 10) + 82. \end{aligned}$$

Proof. Consider the polyomino chain B^1_α with α squares and $\beta = 2$ segments, where $S1$ and S_2 are the two segments satisfying $l_1 = 2$ and $l_2 = \alpha - 1$, respectively, for $\alpha \geq 3$. The five mutually disjoint subsets $\varpi_{2,2}, \varpi_{2,3}$, $\varpi_{2,4}$, $\varpi_{3,3}$ and $\varpi_{3,4}$ can form a partition for $\varpi(B^1_\alpha)$, such that $\varpi(B^1_\alpha(\alpha \geq 3)) = \varpi_{2,2} \cup \varpi_{2,3} \cup \varpi_{2,4} \cup \varpi_{3,3} \cup \varpi_{3,4}$. Further, $|\varpi_{2,2}| = 2$, $|\varpi_{2,3}| = 5$, $|\varpi_{2,4}| = 1$, $|\varpi_{3,3}| = 3\alpha - 10$ and $|\varpi_{3,4}| = 3$. Such that $|\varpi(B^1_\alpha(\alpha \geq 3))| = |\varpi_{2,2}| + |\varpi_{2,3}| + |\varpi_{2,4}| + |\varpi_{3,3}| + |\varpi_{3,4}|$. Therefore, using Eqs. (1)-(2), we arrive at the desired result. □

Theorem 15. *Consider the polyomino chain B^2_α with α squares and β segments, where $S1, S_2, \ldots, S_\beta$ are the segments satisfying the conditions $l_1 = l_\beta = 2$ and $l_2, l_3, \ldots, l_{\beta-1} \geq 3$ for $\alpha \geq 4$. Then, we have the following:*

$$\begin{aligned} SO(B^2_\alpha) &= \sqrt{18}(3\alpha - 6\beta + 3) + 5(4\alpha - 6) + 2\sqrt{13}\beta + 2\sqrt{8} + 2\sqrt{20}, \\ SO'(B^2_\alpha) &= 9(3\alpha - 6\beta + 3) + 12(4\alpha - 6) + 12\alpha + 24. \end{aligned}$$

Proof. Consider the polyomino chain B^2_α with α squares and β segments, where $S1, S_2, \ldots, S_\beta$ are the segments satisfying $l_1 = l_\beta = 2$ and $l_2, l_3, \ldots, l_{\beta-1} \geq 3$ for $\alpha \geq 4$. The five mutually disjoint subsets $\varpi_{2,2}, \varpi_{2,3}$, $\varpi_{2,4}$, $\varpi_{3,3}$ and $\varpi_{3,4}$ can form a partition for $\varpi(B^2_\alpha)$, where $\varpi(B^2_\alpha(\alpha \geq 4)) = \varpi_{2,2} \cup \varpi_{2,3} \cup \varpi_{2,4} \cup \varpi_{3,3} \cup \varpi_{3,4}$. Further, $|\varpi_{2,2}| = 2$, $|\varpi_{2,3}| = 2\beta$, $|\varpi_{2,4}| = 2$, $|\varpi_{3,3}| = 3\alpha - 6\beta + 3$ and $|\varpi_{3,4}| = 4\alpha - 6$. Such that $|\varpi(B^2_\alpha(\alpha \geq 3))| = |\varpi_{2,2}| + |\varpi_{2,3}| + |\varpi_{2,4}| + |\varpi_{3,3}| + |\varpi_{3,4}|$. Therefore, using Eqs. (1)-(2), we arrive at the desired result. □

Theorem 16. *Consider a triangular benzenoid graph T_p, where p denotes the number of hexagons in the base graph. The total number of hexagons in T_p is given by the formula $\frac{p(p+1)}{2}$. Then, we have*

$$\begin{aligned} SO(T_p) &= 6\sqrt{13}(p - 1) + \sqrt{8}\left(\frac{3p(p - 1)}{2}\right) + 6\sqrt{8}, \\ SO'(T_p) &= 36(p - 1) + \frac{27p(p - 1)}{2}. \end{aligned}$$

Proof. Consider a triangular benzenoid graph T_p, where p denotes the number of hexagons in the base graph, and the total number of hexagons in T_p is given by $\frac{p(p+1)}{2}$. The three mutually disjoint subsets $\varpi_{2,2}, \varpi_{2,3}$, and $\varpi_{3,3}$ can form a partition for $\varpi(T_p)$, such that $\varpi(T_p) = \varpi_{2,2} \cup \varpi_{2,3} \cup \varpi_{3,3}$. Further, we have $|\varpi_{2,2}| = 6$, $|\varpi_{2,3}| = 6(p-1)$, and $|\varpi_{3,3}| = \frac{3p(p-1)}{2}$. Therefore, we can compute the total number of edges in T_p as $|\varpi(T_p)| = |\varpi_{2,2}| + |\varpi_{2,3}| + |\varpi_{3,3}|$. Thus, using Eqs. (1)-(2), we arrive at the desired result. □

Theorem 17. *The $SO(X_p)$ is given by*

$$\begin{aligned} SO(X_p) &= 4\sqrt{13}(3p-4) + \sqrt{18}(3p^2-3p+4) + 8\sqrt{8}, \\ SO(X_p) &= 24(3p-4) + 9(3p^2-3p+4) + 32. \end{aligned}$$

Proof. Consider a benzenoid hourglass graph X_p. The three mutually disjoint subset $\varpi_{2,2}, \varpi_{2,3}$ and $\varpi_{3,3}$ can form a partition for $\varpi(X_p)$, where $\varpi(X_p) = \varpi_{2,2} \cup \varpi_{2,3} \cup \varpi_{3,3}$. Further, $|\varpi_{2,2}| = 8$, $|\varpi_{2,3}| = 4(3p-4)$ and $|\varpi_{3,3}| = 3p^2 - 3p + 4$. Such that $|\varpi(X_p)| = |\varpi_{2,2}| + |\varpi_{2,3}| + |\varpi_{3,3}|$. Therefore, using Eqs. (1)-(2), we arrive at the desired result. □

Theorem 18. *The $SO(B_{p,q})$ for $p, q \in \mathbb{N} - \{1\}$ is given by*

$$\begin{aligned} SO(B_{p,q}) &= \sqrt{8}(2q+4) + \sqrt{13}(4p+4q-4) + \sqrt{18}(6pq+p-5q-4), \\ SO'(B_{p,q}) &= 4(2q+4) + 6(4p+4q-4) + 9(6pq+p-5q-4). \end{aligned}$$

Proof. Consider a jagged rectangle benzenoid system, denoted by $B_{p,q}$, where $p, q \in \mathbb{N} - \{1\}$. The three mutually disjoint subsets $\varpi_{2,2}, \varpi_{2,3}$, and $\varpi_{3,3}$ can form a partition for $\varpi(B_{p,q})$, such that $\varpi(B_{p,q}) = \varpi_{2,2} \cup \varpi_{2,3} \cup \varpi_{3,3}$. Furthermore, we have $|\varpi_{2,2}| = 2q+4$, $|\varpi_{2,3}| = 4p+4q-4$, and $|\varpi_{3,3}| = 6pq+p-5q-4$. Therefore, we can compute the total number of edges in $B_{p,q}$ as $|\varpi(B_{p,q})| = |\varpi_{2,2}| + |\varpi_{2,3}| + |\varpi_{3,3}|$. Thus, using Eqs. (1)-(2), we arrive at the desired result. □

4. Conclusion

In this paper we have initiated the study of new topological indices and they are called invariants of Sombor index. The correlation of Sombor index with other variants of Sombor index shows that these Sombor type invariants have equal potential like Sombor index. Finally, we have obtained explicit formulae for the set of nanostructures as well as dendrimers. The mathematical properties of Sombor type invariants remain open for the further study.

Bibliography

[1] Gutman, I. (2021). Geometric approach to degree-based topological indices: Sombor indices. *MATCH Communications in Mathematical and in Computer Chemistry, 86*(1), 11-16.

[2] Harary, F. (1969). *Graph Theory*, Addison–Wesely, Reading.

[3] Gutman, I., & Trinajstić, N. (1972). Graph theory and molecular orbitals. Total π-electron energy of alternant hydrocarbons, *Chemical Physics Letters, 17*(4), 535-538.

[4] Gutman, I. (2013). Degree-based topological indices. *Croatica Chemica Acta, 86*(4), 351-361.

[5] Gutman, I., Furtula, B., & Elphick, C. (2014). Three new/old vertex-degree-based topological indices. *MATCH Communications in Mathematical and in Computer Chemistry, 72*, 616–632.

[6] Li, X., & Zheng, J. (2005). A unified approach to the extremal trees for different indices. *MATCH Communications in Mathematical and in Computer Chemistry, 54*(1), 195-208.

[7] Nadeem, M. F., Zafar, S., & Zahid, Z. (2016). On topological properties of the line graphs of subdivision graphs of certain nanostructures. *Applied Mathematics and Computation, 273*, 125-130.

[8] Ranjini, P. S., Lokesha, V., & Cangül, I. N. (2011). On the Zagreb indices of the line graphs of the subdivision graphs. *Applied Mathematics and Computation, 218*(3), 699-702.

[9] Su, G., & Xu, L. (2015). Topological indices of the line graph of subdivision graphs and their Schur-bounds. *Applied Mathematics and Computation, 253*, 395-401.

[10] Randić, M. (1993). Novel molecular descriptor for structure—property studies. *Chemical Physics Letters, 211*(4-5), 478-483.

[11] Gao, W., Jamil, M. K., Javed, A., Farahani, M. R., & Imran, M. (2018). Inverse sum indeg index of the line graphs of subdivision graphs of some chemical structures. *UPB Scientific Bulletin, Series B: Chemistry and Materials Science, 80*, 97-104.

[12] Ahmad, M. S., Nazeer, W., Kang, S. M., Imran, M., & Gao, W. (2017). Calculating degree-based topological indices of dominating David derived networks. *Open Physics, 15*(1), 1015-1021.

[13] Kang, S. M., Zahid, M. A., Virk, A. U. R., Nazeer, W., & Gao, W. (2018). Calculating the degree-based topological indices of dendrimers. *Open Chemistry, 16*(1), 681-688.

[14] Kwun, Y. C., Farooq, A., Nazeer, W., Zahid, Z., Noreen, S., & Kang, S. M. (2018). Computations of the M-Polynomials and Degree-Based Topological Indices for Dendrimers and Polyomino Chains. *International Journal of Analytical Chemistry, 2018*(1), 1709073.

[15] Kwun, Y. C., Ali, A., Nazeer, W., Ahmad Chaudhary, M., & Kang, S. M. (2018). M-polynomials and degree-based topological indices of triangular, hourglass, and jagged-rectangle benzenoid systems. *Journal of Chemistry, 2018*(1), 8213950.